Active Preview Suspension System
ABC Prescan in the F700

It is good to know what might be happening. This complies with the experiences of real life: Knowing what is approaching supports planning as well as intelligent assignment of resources. This also applies to technology: Regarding the chassis knowing the conditions of the road ahead is useful. A closer look at the active preview system known as Pre-Scan will be taken, which was presented at the 2007 IAA International Motor Show in Frankfurt (Germany) in the F700. It will be examined how the system uses laser scanners to sense the road ahead and guarantees a benefit of comfort through an integral concept of chassis control and Pre-Scan control.

1 Introduction

By implementing the right strategy, it is possible to precondition an active suspension system to the situation ahead. Such anticipative priming of the suspension means that the system need not wait until the vehicle actually meets a rough spot before responding, but can respond instantaneously or even proactively. This translates into greater ride comfort and a whole new driving experience for vehicle occupants. The preconditions for implementing a preview type of suspension control (called Pre-Scan) are advantageous. The Active Body Control (ABC) system [1], the first active suspension system installed in a series production vehicle, has been used since 1999 to counteract sprung mass vibrations through the use of four hydraulic cylinders. At the same time, the quality of the technology used to sense the vehicle surroundings continues to improve. The key factor driving efforts to produce the perfect environment sensing system is the Vision of Accident-free Driving [2]. A closer look at the active preview system known as Pre-Scan will be taken, which was first presented to the public at the 2007 IAA International Motor Show in Frankfurt (Germany) in the F700 research vehicle. It will be examined how the system uses laser scanners to sense the road ahead and look at how a proposed integration of ABC and Pre-Scan can produce even greater comfort. A summary of the knowledge gained from the results of prototype testing will be given at the end.
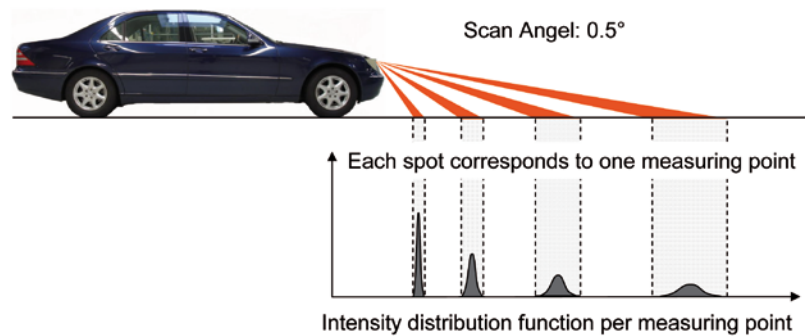
2 Height Profile Estimation

The Pre-Scan concept relies on the ability of the system to produce height profiles of the road surface to the fore of the vehicle's front wheels. For this purpose, two laser sensors are installed in the vehicle's headlamps. These sensors emit beams (spots) with a scan angle of 0.5 degrees, **Figure 1**. Variances in the angle of incidence mean that the spots will exhibit different magnitudes of spread on the road surface. For each individual spot i the laser sensor system delivers a polar distance value D_i. Since the vehicle body's autonomous move-

ments produce variances in the angle of incidence of the spots and hence in the polar distance values, the reconstruction algorithm requires a precise determination of the body position with respect to the road surface in order to compensate for this measurement error. The orientation of the sensor in relation to the road surface is given by the vertical clearance z_{AF} and the pitch angle n_{AF}. One polar distance value D_i along with the associated angle $n_i + n_{AF}$ can be used to calculate the Cartesian distance x_i and height z_i for the spot i, Eq. (1), Eq. (2), **Table**:

$$x_i = (D_i + D_{Off}) \cdot \cos (n_i + n_{AF}) + x_{Korr} (v_x, \Delta T) \quad \text{Eq. (1)}$$

$$z_i = (D_i + D_{Off}) \cdot \sin (n_i + n_{AF}) + z_{AF} \quad \text{Eq. (2)}$$

The Author

Dr.-Ing. Ralph Streiter is a member of the research team at Active Suspensions, Group Research and Advanced Engineering, Daimler AG in Sindelfingen (Germany).

Figure 1: Laser sensors scan the road surface profile. An individual distribution function is assigned to each spot

Table: Variables declaration

$x_{Korr} (v_x, \Delta_t)$	Spatial correction term
D_{Off}	Measurement error offset by diffuse reflection changes on different reflective surfaces
Θ_A	Mass matrix
K_D	Damping matrix
K_F	Spring matrix
z	Body position
n	Pitch angle
w	Roll angle
$\begin{pmatrix} z \\ n \\ w \end{pmatrix}_{Road}$	Modal road surface coordinates
u_{ABC}	Controller output variable
$\begin{pmatrix} z_{rel} \\ n_{rel} \\ w_{rel} \end{pmatrix}$	Measured modal relative coordinates of the body compared to a road compensation surface through the four wheel contact points
$\begin{pmatrix} \ddot{z} \\ \ddot{n} \\ \ddot{w} \end{pmatrix}$	Measured modal accelerations of the body

$x_{Korr}(v_x, \Delta T)$ takes into account a spatial correction of the spots in longitudinal direction correlated to the driving speed as well as to cycle and latency periods of measurement data acquisition. Therefore Equations 1 and 2 transform the polar distance values into a Cartesian profile. Because the required measurement accuracy and reliability can only be attained through the use of statistical calculation, [4] proposes a method for computing the road profile using weighted averaging and iterative recursive reconstruction. To this end, the non-equidistant distance and height values, x_i and z_i, are distributed on an equidistant path grid, thus plotting their positions. Depending on the x-coordinate x_i of the spot i, the spot is assigned a path-equidistant distribution function based on its distance from the vehicle, Figure 1, bottom. The weighted averaging of adjacent and overlapping spots results in an initial estimation for the height profile. Using this estimation, regression can be done using the observed height profile (from the preceding step) to compute a height and pitch angle correction. In this way, an iteration rule can be defined for z_{AF} and n_{AF}. The correction values for z_{AF} and n_{AF} are used to produce an improved estimation of the current profile. This estimation is then used together with the previously reconstructed height profile (taking the associated weightings into account) to produce a new profile estimation. Here, the scan data from the previous measurement cycle are now linked to the current data. The next step is to take the computed profile and, in consideration of the distance travelled, mathematically move the profile against the direction of travel and underneath the car. If the distance travelled is such that the vehicle travels over a road surface profile that has been previously scanned by the laser sensors with sufficient precision, the spatial orientation of the computed road surface profile will be adapted to the current position of the vehicle. This allows for a differentiation between the slope of the road surface and the inclination of the vehicle. The end of one computation cycle marks the beginning of renewed data acquisition by the laser sensors. In the iteration cycle that follows, new data are statistically added to the previous road profile and changes of vehicle position caused by its own
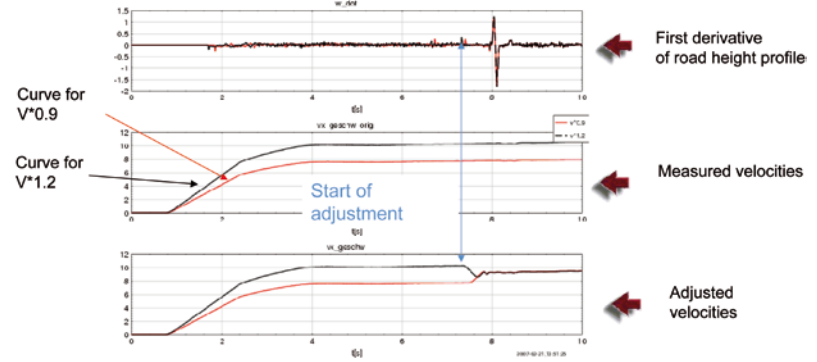

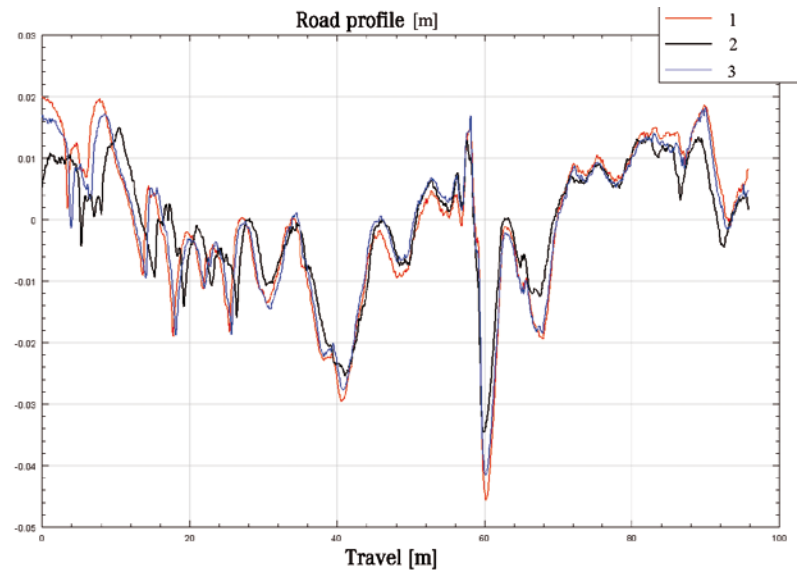**Figure 2:** Velocity adjustment ensures the correct timing for the derivative calculation

Figure 3: Comparison of three measurements taken while driving over the same road surface profile
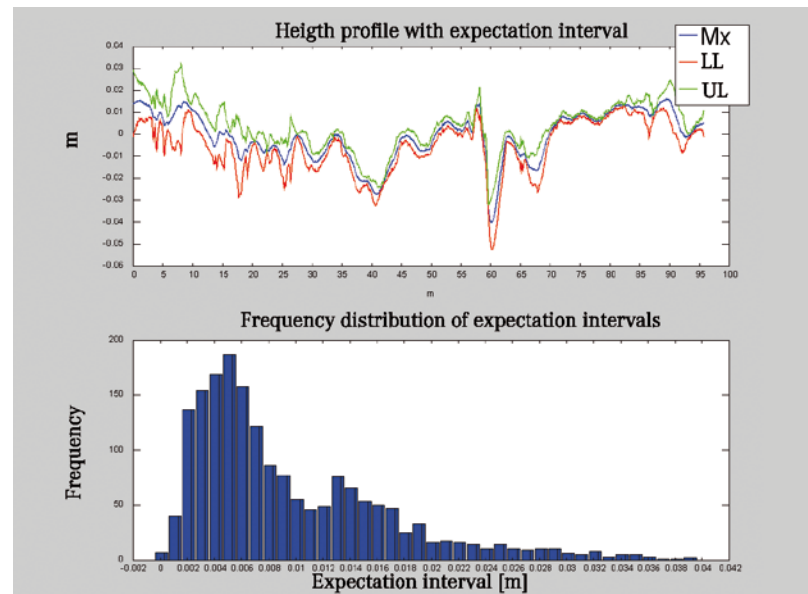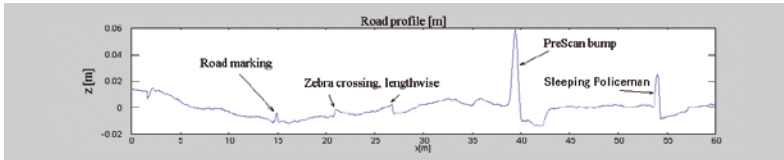

Figure 4: The expectation interval forms an error corridor around the profile. The frequency distribution shows that most errors are less than 1 mm

Figure 5: Road surface height reconstruction can also sense low profile obstacles. The Pre-Scan bump (Figure 8) is detectable at 40 m

movement are determined and compensated for. As iteration continuous, the accuracy of the road profile estimation increases. In the end, the method produces a height profile estimation with spatially distributed error information used to assess the reliability of the data.

3 Velocity Adjustment Through Correlation Analysis

The velocity of the vehicle determines the timing for intervention by the Pre-Scan system. Should this timing go awry, any advantage gained through Pre-Scan could become a disadvantage. Knowledge of the correct vehicle speed is therefore essential if the Pre-Scan strategy is to produce the desired results. Unfortunately, velocity measurement by means of conventional systems such as the antilock brake system (ABS) is not sufficiently accurate and cannot correct for adjustment errors. Based on the consideration that consecutive laser sensor data records depict the same road surface profile and that an x-displacement of the reconstructed road surface profile must be dependent on the vehicle velocity, an autonomous velocity adjustment is integrated into the reconstruction concept. To this end, the system examines the correlation between two consecutive estimated profiles that are mathematically displaced in the longitudinal direction. If the directional tendency is clear, this correlation is then used as a velocity correction factor for an iteration process. The determined direction of displacement as well as the cycle and latency periods of measurement data acquisition must be taken into account here. **Figure 2** illustrates the iteration process using two example trial scenarios. An error factor is assigned to each measured vehicle velocity, Figure 2, centre. At the start of adjustment, the two velocities converge to the same, correct velocity curve, Figure

2, bottom. This method ensures that the first derivative of the road surface profile is indeed computed synchronously, Figure 2, top. Knowing the vehicle velocity is here not only critical for the timing of Pre-Scan interventions, it is also extremely important for calculating the curvature of the road surface. This is because the vehicle velocity v_x is squared in the calculation of the curvature from the road surface profile $z = z(x(t))$.

4 Accuracy of Surface Height Reconstruction

The ultimate outcome of an intervention by the Pre-Scan system relies on a robust closed-loop suspension control system on the one hand and on an effective Pre-Scan strategy on the other. Just as important, however, is the quality of the road surface height profile estimation. To assess the accuracy of the observed road profile, a test vehicle is driven over the same road surface profile in a number of trials. **Figure 3** shows a comparison of three resulting height profile estimations. On the basis of several measurements, the expectation interval for each point in time is established, **Figure 4**, top. The ex-

ample shows an expectation interval of +/- 1 cm. The frequency distribution, Figure 4, bottom, indicates that most errors are smaller than 1 mm. **Figure 5** shows a road surface height curve produced using the method described above.

5 Closed-Loop Control of the Active Suspension

Closed-loop control is of particular importance for two reasons. Firstly, closed-loop suspension control is the fallback level for Pre-Scan in case the sensing accuracy for the road surface height profile is insufficient. And secondly, the control system must realise a structure in the closed control loop that provides favourable access for the proposed Pre-Scan strategy and effective interaction between ABC and Pre-Scan. Closed-loop suspension control must be developed such as to allow for a frequency reduction and a modal perspective of the closed control loop. The controller should demonstrate filtering behaviour, achieve stationary convergence with respect to jump, ramp and vertical wall driving and enable full determination of the resulting stability behaviour. From [3] we know that the following frequency-reduced model can be found for a vehicle with ABC suspension struts, Eq. (3), Table:

$$(\Theta_A \cdot s^2 + K_D \cdot s + K_F)\begin{pmatrix} z \\ n \\ w \end{pmatrix} =$$
$$\frac{1}{s} \cdot u_{ABC} + (K_D \cdot s + K_F) \cdot \begin{pmatrix} z \\ n \\ w \end{pmatrix}_{Road} \qquad \text{Eq. (3)}$$

Taking account of the convergence considerations discussed above for the closed control loop, the following simplified
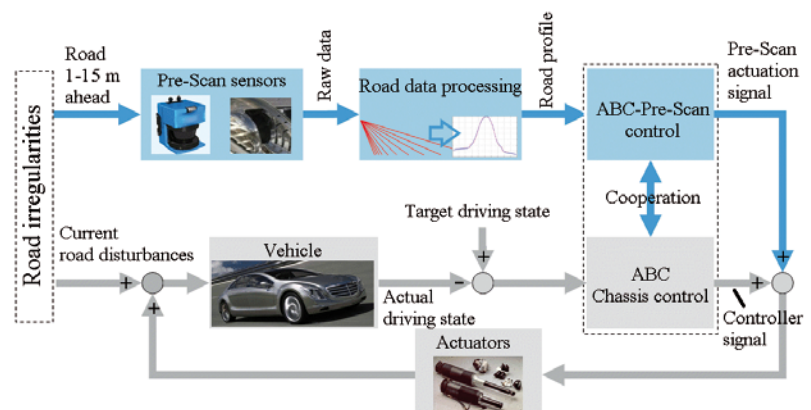
Figure 6: Overall concept for Pre-Scan suspension control

matrix control structure can be selected, Eq. (4) (further control coefficient matrices can provide degrees of freedom and improve the feasibility of the controller)

$$u_{ABC} = [T_4 s^4 + T_3 s^3 + T_2 s^2 + T_1 s + I]^{-1} \cdot$$
$$\left([K_{2B\_R} \cdot s^2 + K_{B\_R} \cdot s] \cdot \begin{pmatrix} \ddot{z} \\ \ddot{n} \\ \ddot{w} \end{pmatrix} + K_{L\_R} \begin{pmatrix} z_{rel} \\ n_{rel} \\ w_{rel} \end{pmatrix} \right) \quad \text{Eq. (4)}$$

with the input measurements, Table.

This leads to the following matrix equation for the closed control loop, Eq. (5):

$$- K_{L\_R}^{-1} [(T_4 s^4 + T_3 s^3 + T_2 s^2 + T_1 s + I)(\Theta_A \cdot s^3 + K_D \cdot$$
$$s^2 + K_F \cdot s) - K_{2B\_R} \cdot s^4 - K_{B\_R} \cdot s^3 - K_{L\_R}] \cdot \begin{pmatrix} z \\ n \\ w \end{pmatrix} =$$
$$= - K_{L\_R}^{-1} [(T_4 s^4 + T_3 s^3 + T_2 s^2 + T_1 s + I) \cdot$$
$$(K_D \cdot s^2 + K_F \cdot s) - K_{L\_R}] \cdot \begin{pmatrix} z \\ n \\ w \end{pmatrix}_{Road} \quad \text{Eq. (5)}$$

The denominator represents the stability behaviour. For this matrix polynomial a desired polynomial can now be prescribed in the form, Eq. (6):

$$\mu_7 s^7 + \mu_6 s^6 + \mu_5 s^5 + \mu_4 s^4 + \mu_3 s^3 + \mu_2 s^2 + \mu_1 s + I$$
$$\text{Eq. (6)}$$

This desired polynomial should demonstrate a diagonal structure while at the same time be oriented to the dynamic behaviour of the non-controlled system in order to enable an interaction be-

Figure 7: Driving over the Pre-Scan bump

tween closed-loop control and roadway [3]. For the closed control loop this results in the desired behaviour as follows, Eq. (7):

$$(\mu_7 s^7 + \mu_6 s^6 + \mu_5 s^5 + \mu_4 s^4 + \mu_3 s^3 + \mu_2 s^2 + \mu_1 s + I) \cdot$$
$$\begin{pmatrix} z \\ n \\ w \end{pmatrix} = - K_{L\_R}^{-1} [(T_4 s^4 + T_3 s^3 + T_2 s^2 + T_1 s + I) \cdot$$
$$(K_D \cdot s^2 + K_F \cdot s) - K_{L\_R}] \cdot \begin{pmatrix} z \\ n \\ w \end{pmatrix}_{Road} \quad \text{Eq. (7)}$$

Comparing the matrix coefficients allows us to establish the control coefficient matrices, Eq. (8):

$$\begin{pmatrix} T_4 \\ T_3 \\ T_2 \\ T_1 \\ K_{2B\_R} \\ K_{B\_R} \\ K_{L\_R} \end{pmatrix}^T \begin{vmatrix} 0 & \Theta_A & K_A & K_F & 0 & 0 & 0 & 0 \\ 0 & 0 & \Theta_A & K_D & K_F & 0 & 0 & 0 \\ 0 & 0 & 0 & \Theta_A & K_D & K_F & 0 & 0 \\ 0 & 0 & 0 & 0 & \Theta_A & K_D & K_F & 0 \\ 0 & 0 & 0 & 0 & 0 & \Theta_A & K_D & K_F \\ -\Theta_A & 0 & 0 & 0 & -I & 0 & 0 & 0 \\ -K_D & 0 & 0 & 0 & 0 & -I & 0 & 0 \\ -K_F & \mu_7 & \mu_6 & \mu_5 & \mu_4 & \mu_3 & \mu_2 & \mu_1 \end{vmatrix} \quad \text{Eq. (8)}$$

The controller as computed here achieves a decoupling of the autonomous dynam-

ics. Numerator diagonalisation is approached but not achieved.

6 Pre-Scan Control (PSC)

The feasibility of the Pre-Scan concept is central to achieving a working suspension system with preview capability. The most obvious approaches involve the direct inversion of the wheel dynamics and hence a complete or partial compensation for road unevenness effected at the wheel. But these approaches are problematic for a number of reasons. First of all, such compensation is parameter sensitive. Algebraic approaches of this type could produce an unintended negative effect on handling up to the level of vehicle instability. Moreover, it would be difficult to organise a sensible interaction with a modal control concept such as is used in the ABC closed-loop control system. The danger exists that closed-loop suspension control and Pre-Scan could act in opposition to one another. Another reason is that a wheel-based compensation system responds more often than is necessary, since the vehicle body has only three degrees of freedom but is borne by four wheels. The resulting fourth degree of freedom is called strain [3] and plays no role with regard to passenger comfort. In a wheel-based compensation system, a road profile characterised by such strain stimuli will produce more activity compared to a body-based Pre-Scan strategy, but without achieving any increase in comfort. As such, the modal, body-based approach is preferred over other approaches for reasons of energy efficiency and robustness. For these reasons, a modal PSC is proposed. Eq. (9) for the closed control loop is used here as a basis for the control system proposal. This approach ensures the harmonious interaction between PSC and ABC control. If

$$u_{ABC} := u_{ABC} + u_{Preview} \quad \text{Eq. (9)}$$

is used n the equation for the frequency-reduced model, the resulting Eq. (10) for the closed control loop is:

$$(\mu_7 s^7 + \mu_6 s^6 + \mu_5 s^5 + \mu_4 s^4 + \mu_3 s^3 + \mu_2 s^2 + \mu_1 s + I) \cdot$$
$$\begin{pmatrix} z \\ n \\ w \end{pmatrix} = - K_{L\_R}^{-1} [(T_4 s^4 + T_3 s^3 + T_2 s^2 + T_1 s + I)$$

Figure 8: The Pre-Scan bump is a 5 cm high and 1 m long ground bump shaped like a sine wave

$$(K_D \cdot s^2 + K_F \cdot s) - K_{L\_R}] \cdot \begin{pmatrix} z \\ n \\ w \end{pmatrix}_{Road} \qquad \text{Eq. (10)}$$

$$- K_{L\_R}^{-1}\,[(T_4 s^4 + T_3 s^3 + T_2 s^2 + T_1 s + I) \cdot u_{Preview}$$

To achieve direct access to the input factors $\begin{pmatrix} z \\ n \\ w \end{pmatrix}_{Road}$, the filter effect of the controller is compensated, Eq. (11):

$$u_{Preview} = (T_4 s^4 + T_3 s^3 + T_2 s^2 + T_1 s + I)^{-1} \cdot K_{L\_R} \cdot u^*_{Preview} \qquad \text{Eq. (11).}$$

This compensation is non-critical, since all coefficients from the controller proposal are precisely known. This compensation share forms the denominator of the PSC. Eq. (10) simplifies to:

$$(\mu_7 s^7 + \mu_6 s^6 + \mu_5 s^5 + \mu_4 s^4 + \mu_3 s^3 + \mu_2 s^2 + \mu_1 s + I) \cdot$$

$$\begin{pmatrix} z \\ n \\ w \end{pmatrix} = - K_{L\_R}^{-1}\,[(T_4 s^4 + T_3 s^3 + T_2 s^2 + T_1 s + I)$$

$$(K_D \cdot s^2 + K_F \cdot s) - K_{L\_R}] \cdot \begin{pmatrix} z \\ n \\ w \end{pmatrix}_{Road} - u^*_{Preview} \qquad \text{Eq. (12)}$$

This matrix equation is viewed as decouplable. Given the prescribed diagonal structure for the desired polynomial, this is true for the denominator of the system. For the numerator it is only approximately true. Errors produced due to the demand for decouplability do not, however, impair the stability of the system since there is no rebound effect on the numerator. As such, the following scalar Eq. (13) can be indicated for mode ϑ_j:

$$N_{j\_Wish} \cdot \vartheta_j = Z_{j\_Road} \cdot \vartheta_{j\_Road} - u^*_{Preview\_Modus\_\vartheta_j} \qquad \text{Eq. (13).}$$

Using the decoupled equations for the controlled vehicle, a pole-zero cancellation individually for each mode can now be performed. This action is of great importance because it prevents Pre-Scan from counteracting one of the many pole-zero cancellations effected by the closed-loop control system by applying derivative terms of the road surface profile that are required for a pole-zero cancellation. Without pole-zero cancellation, a Pre-Scan intervention would result in a worsening of overall behaviour because previously eliminated motion constituents would re-appear. Although a pole-zero cancellation is seen as critical in control engineering with respect to robustness, it in this case represents a favourable condition because all cancelled poles are stable poles and the effect produced by the system on the driver is more agreeable because the perceived complexity of motion is reduced. At the same time, the overall structure maintains the intended system and robustness properties. First the common polynomial N_{j_g} is factored out, Eq. (15)

$$(N_{j\_g} \cdot N'_{j\_Wish}) \cdot \vartheta_j =$$

$$(N_{j\_g} \cdot Z'_{j\_Road}) \cdot \vartheta_{j\_Road} - u^*_{Preview\_Modus\_\vartheta_j} \qquad \text{Eq. (14)}$$

The PSC is determined by prescribing a scalar desired polynomial $Z^{Wish}_{j\_Road}$ for the numerator term Z'_{j_Road}, Eq. (15).

$$(N_{j\_g} \cdot N'_{j\_Wish}) \cdot \vartheta_j =$$

$$(N_{j\_g} \cdot Z'_{j\_Road}) \cdot \vartheta_{j\_Road} - u^*_{Preview\_Modus\_\vartheta_j} \overset{!}{=}$$

$$(N_{j\_g} \cdot Z^{Wish}_{j\_Road}) \cdot \vartheta_{j\_Road} \qquad \text{Eq. (15)}$$

This is followed by, Eq. (16):

$$u^*_{Preview\_Modus\_\vartheta_j} =$$

$$N_{j\_g} \cdot [Z'_{j\_Road} - Z^{Wish}_{j\_Road}] \cdot \vartheta_{j\_Road} \qquad \text{Eq. (16)}$$

In the next step, a frequency reduction is performed that serves to prevent the occurrence of undesired Pre-Scan activity due to high-frequency interference in ϑ_{j_Road}. The above Eq. (16) thus becomes, Eq. (17):

$$u^*_{Preview\_Modus\_\vartheta_j} =$$

$$N^{red}_{j\_g} \cdot [Z'_{j\_Road} - Z^{Wish}_{j\_Road}]^{red} \cdot \vartheta_{j\_Road} \qquad \text{Eq. (17)}$$

If the compensation proposals for all degrees of freedom are summarised, the Pre-Scan design equation can be inserted in the original equation, Eq. (18):

$$u_{Preview} = (T_4 s^4 + T_3 s^3 + T_2 s^2 + T_1 s + I)^{-1} \cdot$$

$$K_{L\_R} \cdot N^{red}_{j\_g} \cdot [Z'_{Road} - Z^{Wish}_{Road}]^{red} \cdot \begin{pmatrix} z \\ n \\ w \end{pmatrix}_{Road} \qquad \text{Eq. (18)}$$

7 Implementation

The question arises as to how to sensibly define the desired numerator polynomial $Z^{Wish}_{j\_Road}$. Boundary conditions create convergence requirements for the overall system. With the chosen controller structure, the closed control loop already incorporates these requirements. As such, the numerator coefficients of Z'_{j_Road}, which are linked with zeroth, first and second order derivatives, are left unaffected, or may be reduced only at very low velocities. In the general case, the coefficients of $Z^{Wish}_{j\_Road}$ will therefore equal those of Z'_{j_Road} up to the second or third order. For the PSC, this results in a numerator polynomial that does not start applying road profile signals until the second or third derivative. Since it is often the case that the order of the term $N^{red}_{j\_g} \cdot [Z'_{j\_Road} - Z^{Wish}_{j\_Road}]^{red}$ is greater than the order of the numerator $(T_4 s^4 + T_3 s^3 + T_2 s^2 + T_1 s + I)$, hence threatening feasibility, it is possible to exploit the lack of zeroth and first order coefficients to our advantage. Due to a phaseless forward-backward filtering of the determined road profile, the first and second derivatives are computed directly at the four wheel contact points. The numerator de-
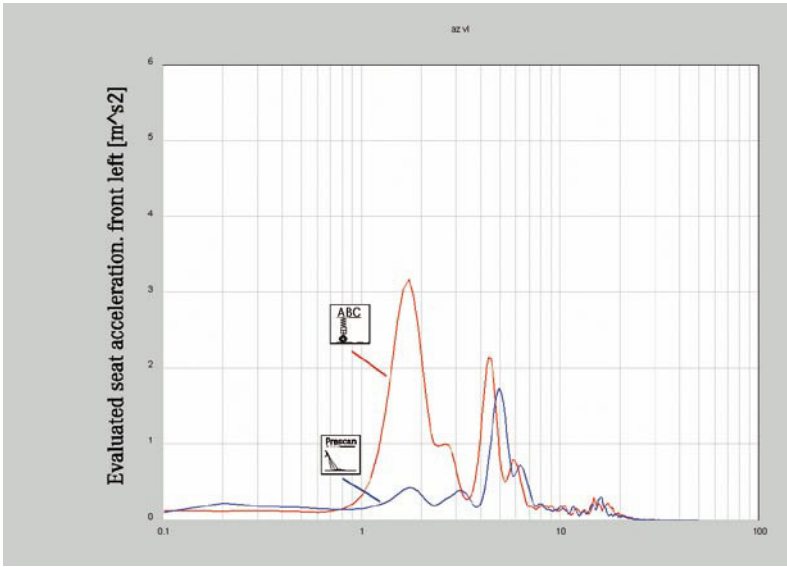
Figure 9: ABC Pre-Scan reduces driver seat acceleration when driving over the Pre-Scan bump
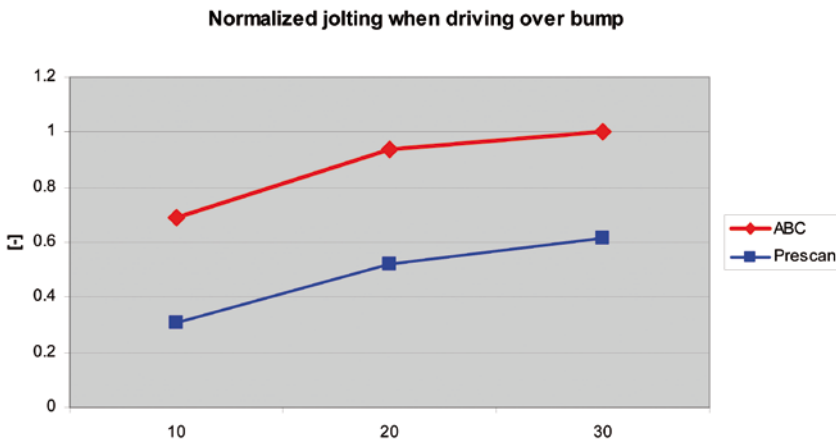

Figure 10: Comparison of normalized jolting at driver seat while driving over bump. Pre-Scan demonstrates its potential at three different velocities
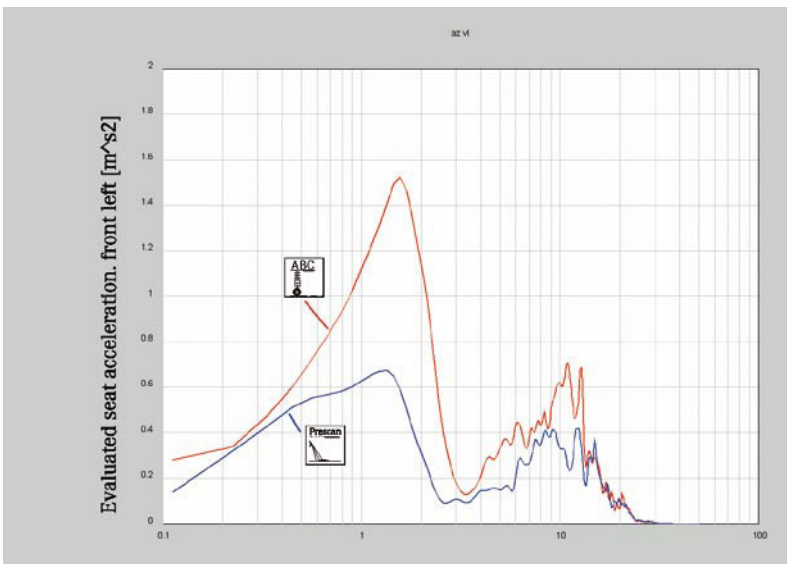

Figure 11: Comparison of evaluated frequency spectra during freeway driving at 100 km/h

gree of the PSC can therefore formally be two orders greater than the denominator degree.

8 Result

In order to study the potential of ABC Pre-Scan, the overall concept, **Figure 6**, was first of all demonstrated in a prototype, **Figure 7**. Taking measurements while driving over the Pre-Scan "bump" allowed us to exploit the full potential, **Figure 8**. The comparison between the frequency spectra of driver seat acceleration evaluated as described in [5] illustrates the improvement in comfort achieved by Pre-Scan, **Figure 9**. **Figure 10** shows the normalised jolt effect (maximum vertical acceleration value) measured at the driver seat at various velocities. The charts shows that when a vehicle with Pre-Scan drives over the bump at 30 km/h, jolting is still less than with ABC at 10 km/h. The advantages of Pre-Scan are clearly evident even on normal road surfaces. **Figure 11** shows the frequency spectrum of driver seat acceleration during freeway driving at 100 km/h. Compared to ABC, Pre-Scan provides added comfort benefits. The benefits are just as great during the "freeway hop" test where the vehicle is jolted by the seams between concrete freeway slabs at regularly recurring intervals. **Figure 12** contrasts the evaluated pitch acceleration values measured at the driver's position. ABC sharply reduces vibration when compared to a vehicle without body control. Pre-Scan can produce a further substantial reduction of acceleration values.

9 Summary

Pre-Scan merges the possibilities offered by active suspension and laser-aided road surface profile sensing into a single function using an integral closed-loop and straightforward control concept. The road surface profile sensing technique is based on a statistical method that uses scan matching to achieve the required degree of observational accuracy and robustness for closed-loop control and that recursively estimates the autonomous vertical vehicle motion, the vehicle velocity and various other sensor corrections. The proposal
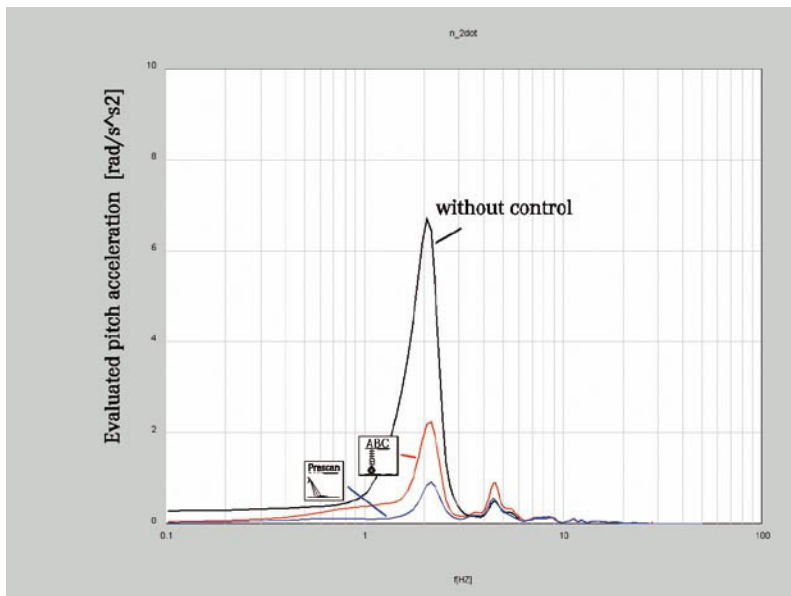
Figure 12: Comparison of evaluated frequency spectra of pitch acceleration during freeway hopping at 40 km/h

for the straightforward Pre-Scan control system is based on a modal perspective of the closed control loop and interacts harmoniously with ABC in accordance with the compensation principle. The result of this synthesis is a clear increase in ride comfort. This approach has been realised in a vehicle for the first time. Measurements and test performed on various road surfaces underscore the potential that Pre-Scan holds. The concept was presented to the public at the IAA 2007 in the F700 research car under the name Pre-Scan Suspension.

References

[1] Wolfsried, S.; Schiffer, W.: ActiveBodyControl. Das neue aktive Federungs- und Dämpfungssystem des CL-Coupé von Mercedes-Benz, VDI-Fachtagung Reifen/Fahrwerk/Fahrbahn, Hanover, 1999
[2] Daimler Chrysler AG: Die Vision vom unfallfreien Fahren, Hightech Report 2001
[3] Streiter, R.: Entwicklung und Realisierung eines analytischen Regelkonzeptes für eine aktive Federung, Dissertation, TU Berlin, 1996
[4] Schindler, A.; Streiter, R.; Bretthauer, G.: Integraler Ansatz für eine Fahrzeugregelung mit Preview, chassis.tech Munich, 2007
[5] Frank, P.: Bewertungsverfahren Schwingempfinden, Daimler Benz AG, Forschungsinstitut F1M, 1994 (94-004), Technischer Bericht